EGYPTIAN ACADEMIC JOURNAL OF

BIOLOGICAL SCIENCES

C

PHYSIOLOGY & MOLECULARBIOLOGY

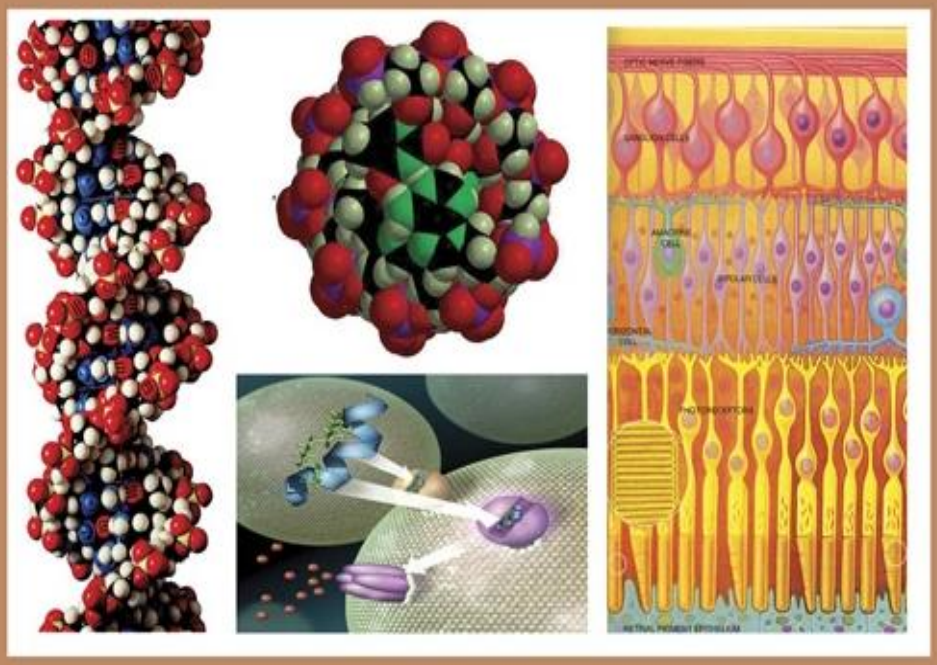

ISSN
2090-0767

WWW.EAJBS.EG.NET

Vol. 15 No. 2 (2023)

.

Citation: *Egypt.Acad.J.Biolog.Sci. (C.Physiology and Molecular biology) Vol. 15(2) pp37-50 (2023)*
DOI: 10.21608/EAJBSC.2023.308857

Egypt. Acad. J. Biolog. Sci., 15(2):37-50 (2023)

Egyptian Academic Journal of Biological Sciences

C. Physiology & Molecular Biology

ISSN 2090-0767

www.eajbsc.journals.ekb.eg

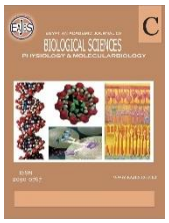

Design, Synthesis, and Anticancer of Some New Amide Derivatives from Coumarin-3-Carboxylic Acid Combined with Carbohydrate

Ruaa W. Adam and Ezzat H. Zimam

Department of Chemistry, Faculty of Science, University of Kufa, Najaf, Iraq

***E-mail:** ruaaw.abdulfadhil@uo.kufa.iq- ezat_ahlam@yahoo.com

ARTICLE INFO

Article History

Received:4/6/2022

Accepted:19/7/2023

Available:23/7/2023

Keywords:

Coumarin-3-Carboxylic acid, Glucose, amide derivatives.

ABSTRACT

A series of new coumarin derivatives based on carbohydrates were designed, and synthesized by employing the so-call 'sugar-tail' approach. The synthesis of amide derivatives involves the first step It includes the reduction of the azide sugar derivatives by hydrogen gas in the presence of activated palladium. The second step includes the reaction of the prepared amine derivatives with the carboxylic coumarin derivative to produce the amide derivatives. All of the compounds showed great water solubility and the pH value of their water solutions of compounds is 7.0. Docking simulation studies were performed to check the binding patterns of the synthesized compounds. The cytotoxicity potentials of 1,2,3-triazole glucosides derivatives were evaluated by MTT assay against liver cancer primary tissue culture after 48 hr., which appears that amide glucosides derivatives exhibited selective cytotoxicity against liver cancer cells isolated from Iraqi patients with inhibitory concentration (IC50) 106.81 µg/ml. Enzyme inhibition assay studies were also conducted for the epidermal growth factor receptor (EGFR), and the results explained the activity of a number of derivatives. All the synthesized compounds were characterized by IR, 1H, 13C NMR and Mass spectroscopy.

INTRODUCTION

Carbohydrate-based low molecular weight gelators (LMWGs) have received increasing attention over recent years due to their interesting physical-chemical properties and many applications(Du *et al.*, 2014)(Zhou *et al.*, 2017). The gelators typically self-assemble and form fibrous supramolecular architectures that can immobilize certain solvents and form reversible gels. The driving forces for the formation of supramolecular gel networks are non-covalent forces such as hydrogen bonding, hydrophobic interactions, p-p stacking, CH-p interactions, and van der Walls forces, etc. Low molecular weight organogelators (LMOGs) have shown numerous applications for the formation of new supramolecular materials(Okesola & Smith, 2016)(Amabilino *et al.*, 2017). Coumarin and its derivatives display a wide variety of biological activities, such as antitumor, anticoagulant, antispasmodic, antidiabetic, antibiotic, anti-HIV-1, and antioxidant activities(Salar *et al.*, 2018)(Emami & Dadashpour, 2015). Interestingly, coumarin-3-carboxylic acids (also known as 3-carboxycoumarins) have some specific applications in a wide range of possibilities over other coumarin derivatives (esters and amides)(Markad *et al.*, 2020)..carboxamides, prevalent in both natural and synthetic molecules, find use as drugs, insecticides, and synthetic or biopolymeric materials.(Pitzer & Steiner, 2016)Their preparation from carboxylic acids and amines is a challenging, high-priority reaction, particularly regarding atom economy(Bryan *et al.*, 2018).

The production of amides directly from carboxylic acids and amines is inhibited by the energy barrier for the dehydration of stable ammonium carboxylate (Ramachandran & Hamann, 2021). Cancer is one of the most serious and complicated health disorders all over the world(El-Sayed *et al.*, 2022). Owing to the incidence of resistance, toxicity, and lack of selectivity of the currently existing anticancer drugs, targeted therapies have recently been approved for the treatment of definite cancers such as lung, breast, pancreatic and colorectal cancers as well as lymphoma and leukemia(Gerber, 2008).

MATERIALS AND METHODS

The melting points were recorded through a Reichert Thermovar apparatus and are uncorrected. The infrared spectra were recorded using a Perkin-Elmer (model 1720) FTIR spectrometer. Nuclear magnetic resonance investigations were performed on a Bruker AC-300 or DPX-300 spectrometer (400 MHz 1H) (100 MHz 13C). The values of ppm (chemical shifts) are reported relative to TMS as a standard reference. The J values (coupling constants) are provided in Hz. The progress of the reaction was checked and guided by TLC using aluminum silica gel 60 F245. IR, 1H NMR, 13C NMR and elemental analyses were measured at the Micro Analytical Center at the Faculty of Science, Basra University, Iraq.

1-Synthesis of ((2R,3S,4S,5R,6R)-3,4,5-trihydroxy-6-methoxytetra hydro-2H-pyran-2-yl) methyl 4-methylbenzenesulfonate (2A)(El-Abid *et al.*, 2021):

Adding 1.2 equiv. of TsCl in a solution of 1equiv.of methyl α-D-glucopyranoside in dry pyridine at 0 °C. The mixture was then gradually warmed up to room temperature. The reactions were monitored by TLC, mass spectrometry and H^1NMR, between 2 and 24 hours of stirring. It is evident that, despite the use of an excess of TsCl. the conversion remains limited and unreacted glucose was still present in a significant amount.

2-Synthesis of 2-Bromoethyl-2,3,4,6-tetra-O-acetyl-β-D glucopyranoside or (2r,3r,4s,5r,6r)-2-(Acetoxymethyl)-6-(2-Bromoethoxy) Tetrahydro-2h-Pyran-3,4,5-Triyl Triacetate (3B)(Yarlagadda *et al.*, 2015):

Penta-O-acetyl-β-D-glucopyranose (b2) (62.45g, 0.16 mol) and 2-bromoethanol (13.9 mL, 0.19 mol) were dissolved in dry CH_2Cl_2 (250 mL) in the dark and cooled to 0°C. $BF_3{\cdot}Et_2O$ (100 mL, 0.81 mol) was then slowly added. The mixture was then stirred at 0°C for 3 h and for 20 h at room temperature. After completion of the reaction, CH_2Cl_2 (50 mL) was added to the mixture, which was then poured into cold water (250 mL) with vigorous stirring. The organic layer was separated and washed repeatedly with water and saturated sodium bicarbonate. The organic phase was dried over anhydrous Na_2SO_4 and concentrated on a rotary evaporator. The resulting residue was purified by flash chromatography (stationary phase: silica gel; mobile phase: 2% methanol in CH_2Cl_2). The product was a white crystalline solid, with a yield of 37.01 g (50%).

3-General Procedure For The Protection Of Hydroxyl Group In Glucopyranoside 3A & 3B (Wang *et al.*, 2010):

The preparation of O-acetyl methyl α-D-glucopyranoside to a cold mixture of 2A&2B (1.0 g) and pyridine (50 mL) was added acetic anhydride (15 mL). The mixture was stirred overnight and then transferred to a separation funnel with EtOAc (50 mL). The solution was washed with 2 N HCl, saturated NaHCO3 and brine, dried over Na_2SO_4 and concentrated to afford 2.263 g of O-acetyl methyl-α-D-glucopyranoside, which was further purified by crystallization in EtOAc/hexane, in almost quantitative yield.

4-General Procedure For The Synthesis of Azide Sugars 4A & 4B (Hao *et al.*, 2020):

(0.01mol) from compound (3A&3B) was dissolved in (15 ml) from DMF and add of 0.01 mol from sodium azide reflex the reaction at 120 C^O, the reaction course was followed by TLC ethyl acetate: hexane as eluent. The crude material was purified by

column chromatography ethyl acetate: hexane and concentrated under a rotary evaporator to give the desired compound.

Chemical Formula(4A): $C_{13}H_{19}N_3O_8$; 80% Yield, The IR spectrum showed the absence of azide absorption band starting in *v* (2101cm^{-1}).

Chemical Formula(4B): $C_{16}H_{23}N_3O_{10}$; 85% Yield, The IR spectrum showed the absence of an azide absorption band starting in *v* (2101cm^{-1}).

5-General procedure for the synthesis of amino sugars 5A and 5B.(de Oliveira *et al.*, 2005):

A solution of azido sugar 4A & 4B (1 mmol) in methanol (5 mL) was stirred under H2 atmosphere (1 atm) for 16 h in the presence of 10% Pd–C. (10% w/w of azido sugar). The catalyst was then removed by filtration and the solvent was evaporated under reduced pressure. The obtained residue was purified by chromatography on Silica Florisil using 4% MeOH in CH_2Cl_2 as the eluent affording the corresponding amino sugar 5A and 5B, respectively.

Chemical Formula (5A): $C_{13}H_{21}NO_8$, the IR spectrum showed the disappearance of azide and the appearance absorption band of amine starting in *v* (3339 cm^{-1}).

Chemical Formula (5B): $C_{16}H_{25}NO_{10}$, the IR spectrum showed the disappearance of azide and the appearance absorption band of amine starting in ν (3386 cm^{-1}).

6- **General procedure for the synthesis of amide sugars 6A and 6B.(Fattahi *et al.*, 2018):**

To a magnetically stirred solution of 3-carboxylic acid coumarin (1 mmol) in chloroform was added 1 mmol of N, N'-diisopropylcarbodiimide and the reaction mixture was stirred at room temperature for 1 h. After this period, the amine (1mmol) was added and the reaction mixture was stirred at room temperature for the indicated time until the starting materials were totally consumed as checked by TLC. Then, the solvent was separated by filtration.

Chemical Formula (6A): $C_{23}H_{25}NO_{11}$, yield 80%, white powder, m.p =190C^o, The IR spectrum showed the disappearance of amine and appearance absorption band of amide bond starting in ν 3316 cm^{-1} (-NH),1642 carbonyl amide. ^{1}H NMR (400 MHz, Chloroform-*d*) δ 9.22 (s, 0H), 8.93 (dd, *J* = 10.3, 7.5 Hz, 0H), 8.01 (s, 1H), 7.87 – 7.65 (m, 1H), 7.65 – 7.50 (m, 1H), 7.47 – 7.29 (m, 2H), 5.12 – 4.73 (m, 1H), 4.34 – 4.03 (m, 1H), 3.62 – 3.35 (m, 3H), 3.39 – 3.20 (m, 1H), 2.97 (s, 2H), 2.89 (s, 2H), 2.45 (d, *J* = 3.0 Hz, 1H), 2.23 – 2.11 (m, 1H), 2.15 – 2.01 (m, 4H), 2.06 – 1.94 (m, 1H), 1.97 – 1.87 (m, 2H), 1.90 – 1.52 (m, 4H), 1.37 (td, *J* = 10.2, 9.1, 4.4 Hz, 1H), 1.35 – 1.27 (m, 1H), 1.15 (ddt, *J* = 50.3, 26.4, 7.0 Hz, 5H) . ^{13}C NMR (101 MHz, $CDCl_3$) δ 157.04, 153.76, 153.18, 125.68, 118.00, 77.38, 77.06, 76.74, 63.01, 61.91, 40.30, 39.69, 33.79, 32.25, 30.71, 29.69, 28.91, 26.23, 26.00, 25.56, 25.26, 25.19, 24.89, 24.57.

Chemical Formula (6B): $C_{26}H_{29}NO_{13}$, yield 85%, white powder, m.p =199C^O, The IR spectrum showed the disappearance of amine and appearance absorption band of amide bond starting in ν 3309 cm^{-1}, 1639 cm^{-1} carbonyl amide.

7-Removal of Protective Groups Synthesis of (7A,7B)(Mohammed *et al.*, 2017):

Compounds (0.3 mmol), were dissolved in methanol (5 mL), and sodium ethoxide (2.04 mg,0.03 mmol) was added thereto. Then the reaction mixture was stirred at room temperature until the disappearance of starting material (6 hours) and concentrated. Then it was extracted with 40 mL of diethyl ether three times and then the organic phase was treated with 100 mL of water (three times). Subsequently, the diethyl ether phase was dried by adding anhydrous sodium sulfate (Na_2SO_4) and then filtered. The diethyl ether was evaporated and then the residue was dried

Chemical Formula(7A): $C_{17}H_{19}NO_8$, yield 75%, light pink, m.p =180C^o**,** The IR spectrum showed ν 3557, 3322 cm^{-1}, 1576 cm^{-1} carbonyl amide.

Chemical Formula(7B): $C_{18}H_{21}NO_9$, yield 80%, pink, m.p =188C^o**,** The IR spectrum showed ν 3409 cm^{-1}, 1613 cm^{-1} carbonyl amide.

Molecular Docking Studies:

On an Intel Xenon W 3565 CPU running Ubuntu business version 14.04, the Glide module of the Schrodinger program was installed, and docking experiments with highly active and moderately active compounds were conducted. The RCSB protein data repository was the chosen source, and it provided the protein structure. The Chemdraw 18.0 Perkinelmer program was used to design the specific ligands.

Ligand Preparation:

ChemDraw was used to clean up the structure for bond alignment and draft the ligands for the docking experiment. Then, to reduce energy as ligands were introduced to the workstation, the OPLS3e (Optimized Potentials for Liquid Simulations) force field was implemented in Ligprep (Version 2019-1, Schrodinger). Since it enables the assignment of bond order, the addition of hydrogens to ligands, and the conversion of the 2D structure to 3D, this minimization is helpful for docking investigations. The best ligand conformations output file was used in docking studies.

Protein Preparation:

The Schrodinger protein preparation wizard (2019-1 version) was the primary protein preparation and minimization tool. The protein had a hydrogen atom added to it, and charges were also assigned. Het states were generated with Epik at a pH of 7.0 2.0. The protein is preprocessed and then refined and modified by evaluating the water molecules and other factors in the working space. The most important water molecules were unaltered, whereas all other molecules save those containing heteroatoms were removed. Finally, the OPLS3 force field was used to achieve maximum protein minimization. Using the ligand that was co-crystallized with the protein of interest (PDB-4GQR), a grid was constructed that represents the active site of the chosen target. Root mean square deviation (RMSD) was used to verify the protein after the last docking step with the co-crystal ligand in XP mode, and the value was found to be in the region of 0.46.

Receptor Grid Generation:

A receptor grid was created around the protein by choosing the inhibitory ligand (X-ray posture of the ligand in the protein; PDB:4GQR). With a partial atomic charge of 0.25, the Vander Waal radii of the receptor atoms were scaled to 1.00, and a box was created around the centroid of the ligand.

Docking and Analysis:

The above-described ligand and protein were used as input in a molecular docking experiment. XP Visualiser (Version 2019- 1, Schrodinger) was used to assess the docking study's findings. The compounds' SMILES format was created with OSIRIS Datawarrior. The Glide module in Schrodinger was used for docking experiments of the planned and produced compounds. We used XP mode (extra precision) for all docking calculations. The protein's atomic weight was reduced by a factor of 0.8, and the atoms had a partial atomic charge of less than 0.15. The best-docked confirmation was selected based on the Glide docking score. XP visualizer was used to delving deeper into the interactions between these docked conformations.

Preparation of Primary Cell culture of true cut Breast Tumor Biopsies: This protocol was adapted from Speirs (2004) and provided by V. Speirs of the Breast Research Group at the Leeds Institute of Molecular Medicine at St. James's University Hospital in Leeds, UK. Under local anesthetic and guided by ultrasound imaging, the oncologist took true-cut samples of the patient's breast tumors and sent them to the cell culture facility.

Preparation Primary True-cutting cell culture Biopsies of the liver and tumor:

Under local anesthetic and guided by ultrasound imaging, oncologists took true-cut biopsies of patients' liver cancers from the tu mor core and sent them on to the cell transpl ant team unit.

- **Primary Cell Exposure To 7A** & **7B**:

Cell suspension with 1×10^5 per ml was transferred to microplate 96-plate wells with each 120 µl well with cell suspension

exposed to various concentrations of 7A & 7B (12.5, 25, 50, 100, 200 µg/ ml). Following that, 50 µl of 7A & 7B were added to each well in triplicate with each concentration and incubated with CO2 for 24 hours.

RESULTS AND DISCUSSION

Synthesis and Identification of Carbohydrate Derivatives:

Using B-D-glucopyranose as a starting material, the synthesis technique involved treating the reaction for 3 hours with TSCl in dry pyridine to generate a first derivative 2A, also in high yield. In order to preserve the hydroxyl group, the product reacts with acetic anhydride in the same solvent, yielding 3A. treated with 2-bromoethanol in dry CH2Cl2 at 0 degrees Celsius in the dark. the second derivatives 1,2,3,4,6- penta-O-acetyl--D-glucopyranose as starting material. For example, BF3+Et2O3B. Both 3A and 3B are introduced into the Due to the potency of the nucleophile (N3), the SN2 reaction with sodium azide in DMF resulted in a high yield of azide carbohydrate from 4A&4B. Amino sugars 5A and 5B are synthesized via the reduction of azide carbohydrate derivatives in a hydrogen peroxide environment (1 atm) in methanol for 16 hours. This section outlines the general synthesis pathway for sugar derivatives. Scheme1.

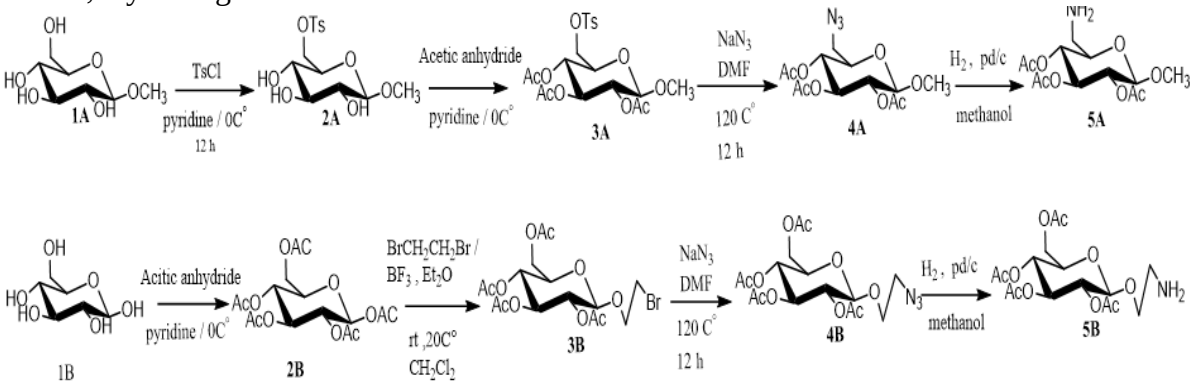

Scheme 1: -synthesis of aminosugar derivatives

Synthesis of Amide Derivatives:

Amide bond formation from coumarin 3-carboxylic acid with aminosugar in CCl_4 present DCC to product 6A&6B respectively. Scheme 2.

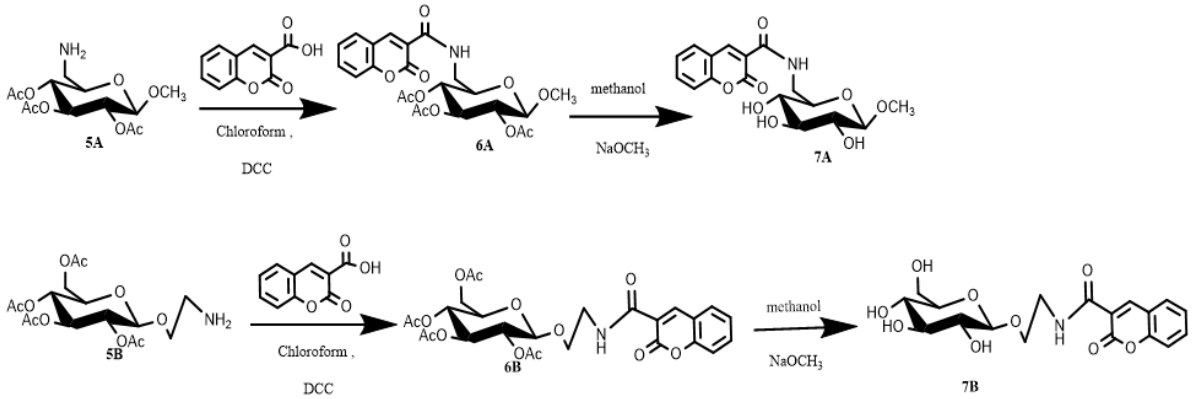

Scheme 2: synthesis of amide sugar derivatives

All the synthesized compounds were characterized by IR, ^{1}H, ^{13}C NMR and Mass spectroscopy. The appearance of the singlet at 8.5-8.6 ppm in ^{1}H NMR confirms the amide NH unit. Figure (1).

One peak appeared around 170 ppm in ^{13}C NMR confirming the presence of carbonyl carbon in all the titled derivatives & Three peaks at 14.47, 11.55 and 10.08 in ^{13}C NMR confirm the isopropyl unit (Fig. 2).

The IR spectrum of compound 6A yet again confirms the presence of carbonyl (1642 cm^{-1}), NH (3316 cm^{-1}) and the IR spectrum of compound 6B yet again confirms the presence of carbonyl (1636 cm^{-1}), NH (3314) cm^{-1}).

The FT-IR of the Removal protection group of compounds 7A & 7B shows, Peak appearance when 3557 ,3409 cm^{-1} due to OH groups.

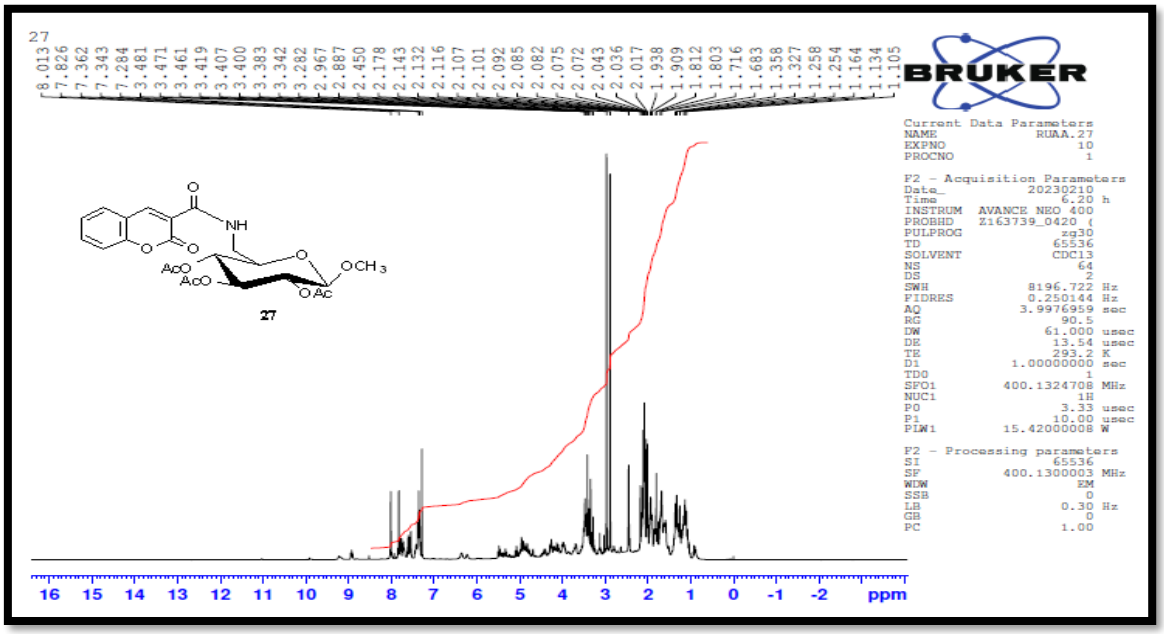

Fig. 1: ^{1}H NMR spectrum of compound 6A**.**

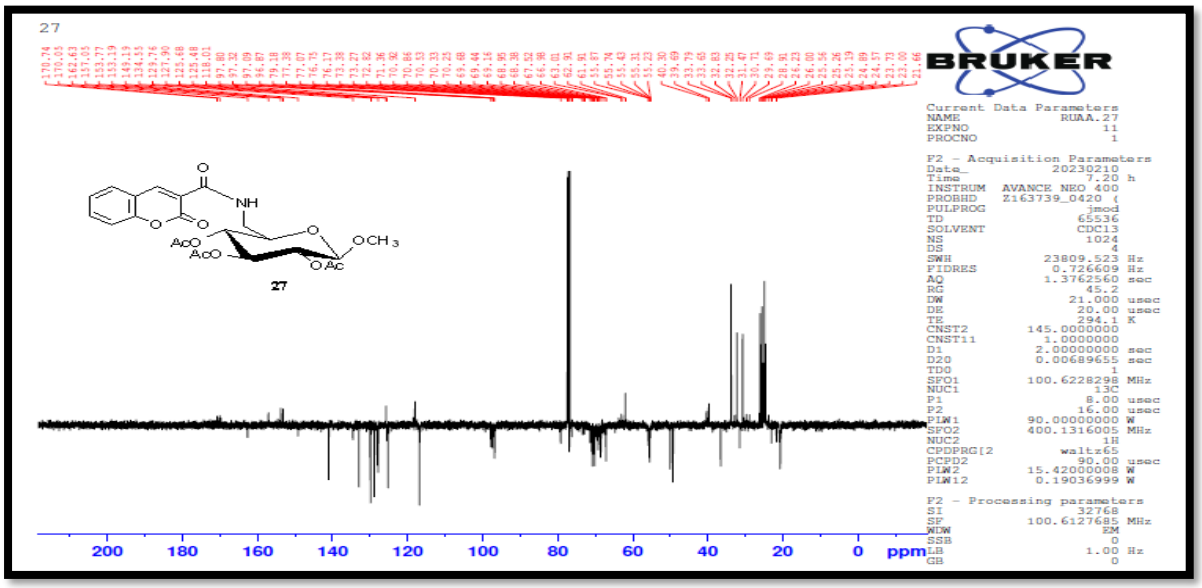

Fig. 2: ^{13}C NMR spectrum of compound 6A.

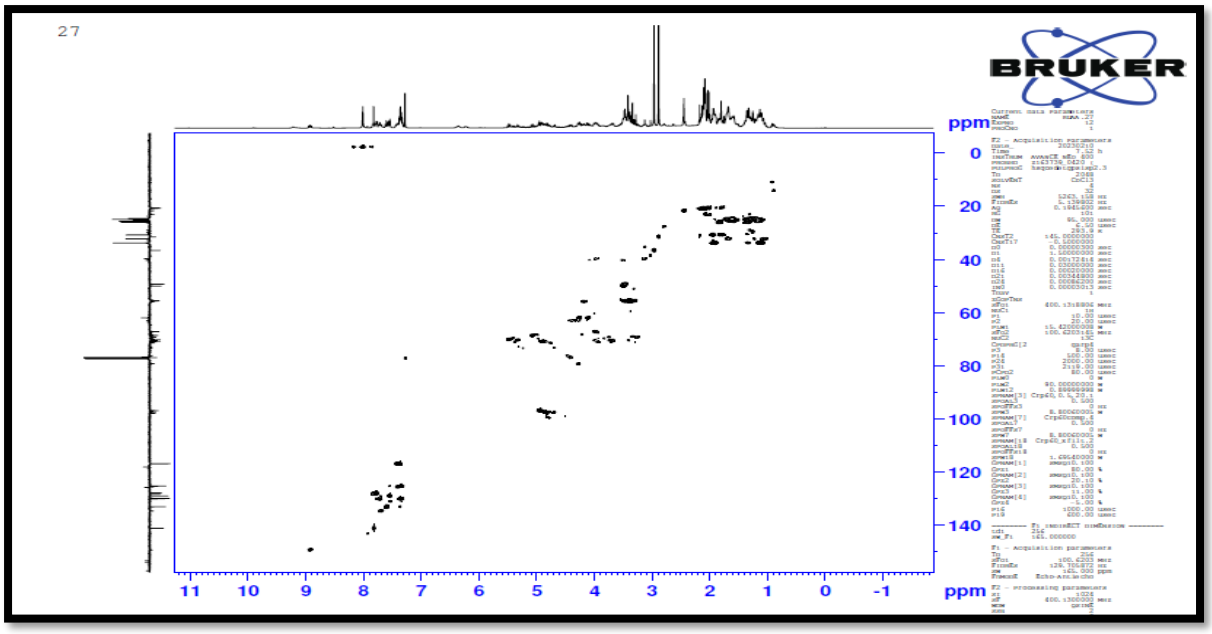

Fig. 3: HSQC of experiment Compound 6A.

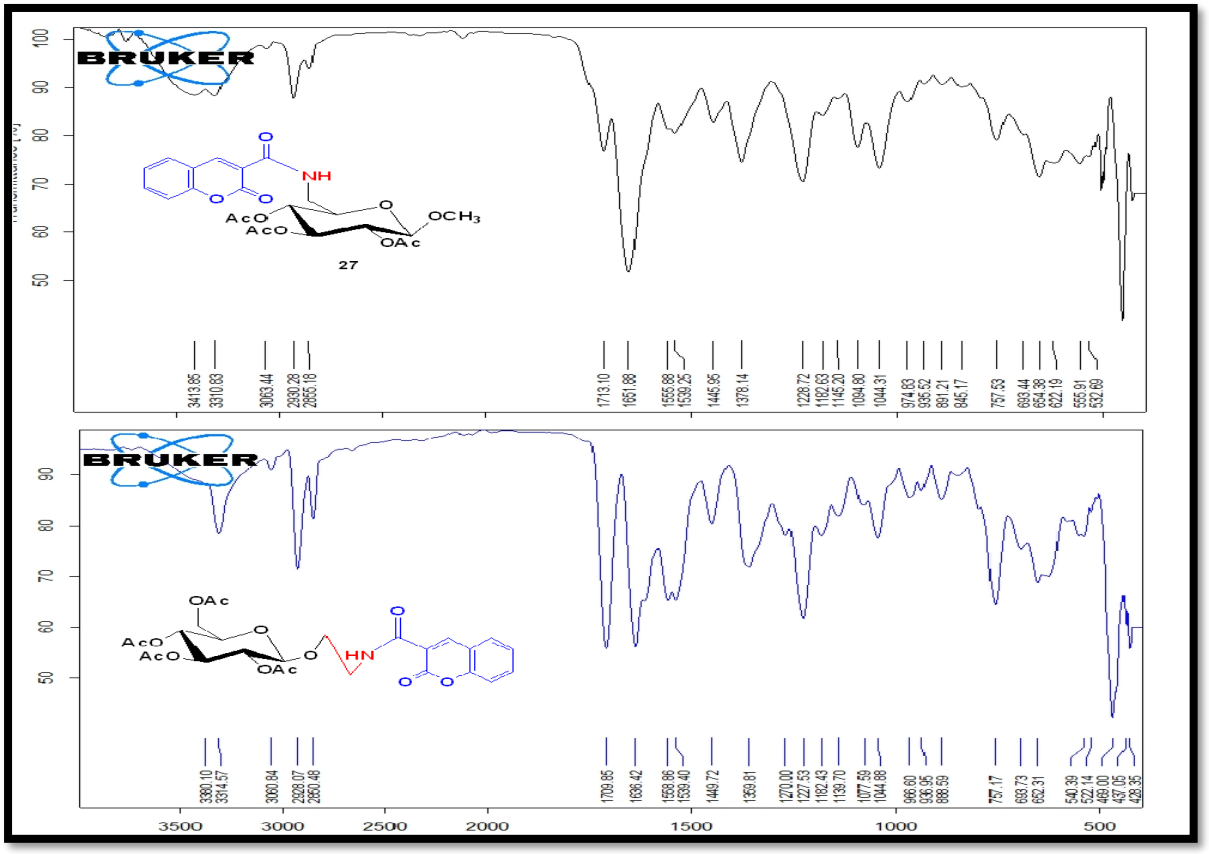

Fig. 4: FTIR spectrum of Compound 6A & 6B.

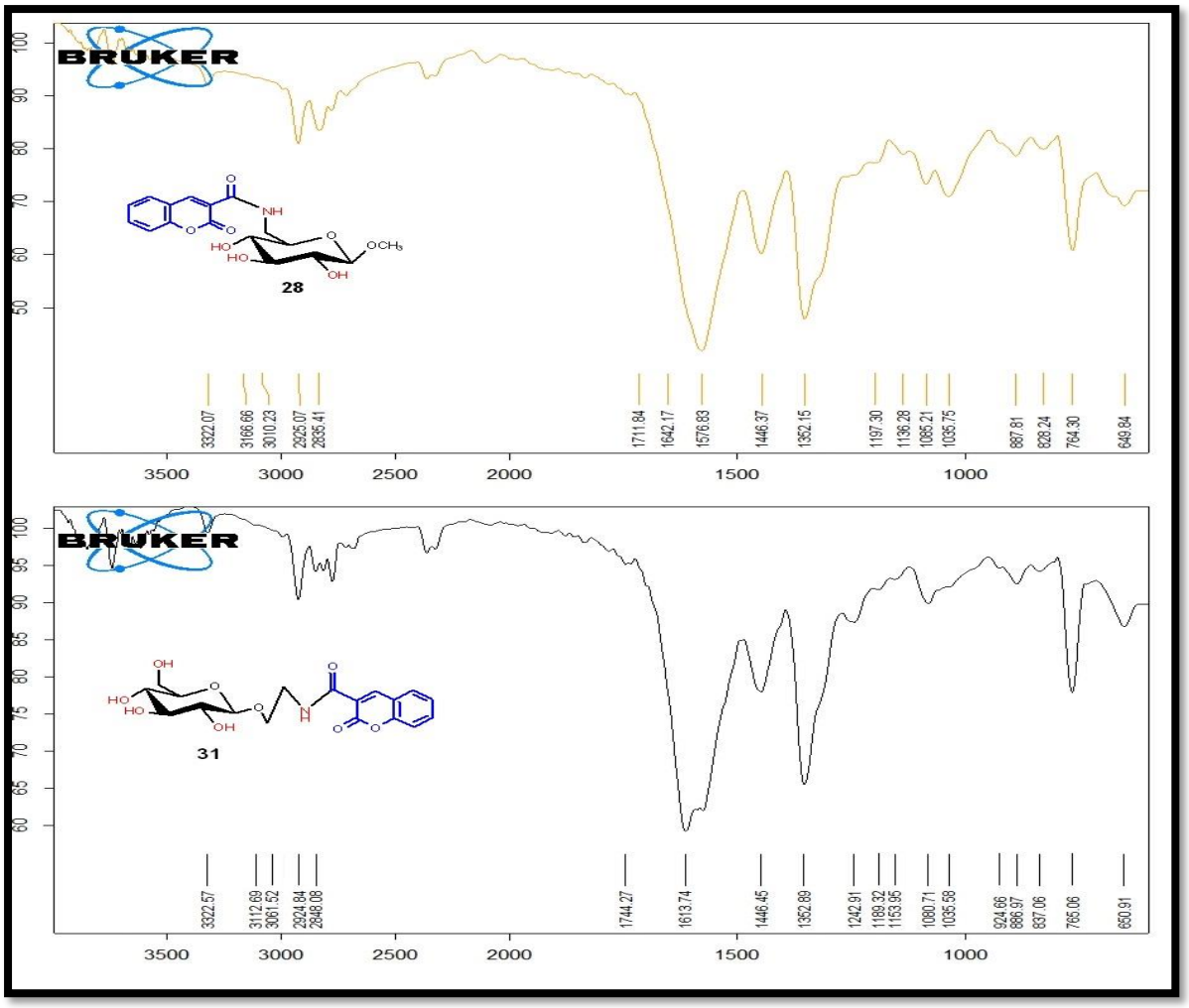

Fig. 5: FTIR spectrum of Compound 7A & 7B.

Molecular Docking Study:

The Molecular Operating Environment (MOE-Dock) software version 2014.0901 was used to do docking simulations for targets 6A, 7A, 6B, and 7B in order to evaluate their promising in vitro inhibitory effects and comprehend their binding mechanisms within the EGFRWT, EGFRT790M, and HER-2 active sites. The Protein Data Bank files for the relevant EGFRWT, EGFRT790M, and HER-2 enzymes (PDB codes: 1M17, 3UG2, and 3RCD, respectively) were selected and downloaded.

Selection Of Protein Crystal Structures:

Crystallographic Structures of Protein:

Mitogen-activated protein kinase (JNK1) are provided in the Protein Data Bank pdb code (A1 chain with) (4AWI). This section evaluates and chooses the 4AWI crystal structure for docking. The MOE structure organization technique corrected the faults in the protein by identifying the biggest and ligand pockets, inserting the tested compounds in these pockets for docking, ligand interaction, computing the total binding energy, and calculating the H-bond and Van der Waals (VDW) energies.

Compound 6A;
S -5.6147, rmsd-refine 1.2931
Ligand Interactions Report

Ligand	Receptor	Interaction	Distance	E (kcal/mol)
O 43	ND2 ASN 156 (A)	H-acceptor	3.57	-0.7
6-ring	CG1 VAL 158 (A)	pi-H	4.36	-0.6

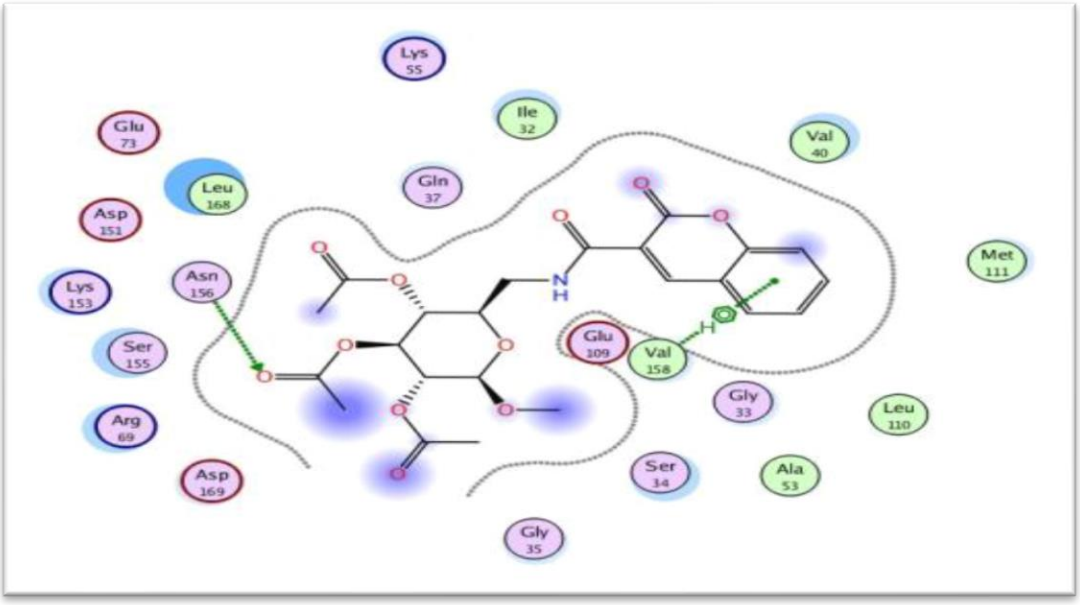

Fig. 6: Compound 6A.

Compound 7A ;
S -5.3186, rmsd-refine 1.8160
Ligand Interactions Report

Ligand	Receptor	Interaction	Distance	E (kcal/mol)
O 12	SD MET 108 (A)	H-donor	3.58	-2.0
O 41	SD MET 108 (A)	H-donor	3.47	-1.0
O 39	NE ARG 69 (A)	H-acceptor	3.21	-0.7
O 39	NH2 ARG 69 (A)	H-acceptor	2.92	-1.5
6-ring	N ALA 36 (A)	pi-H	4.59	-0.6

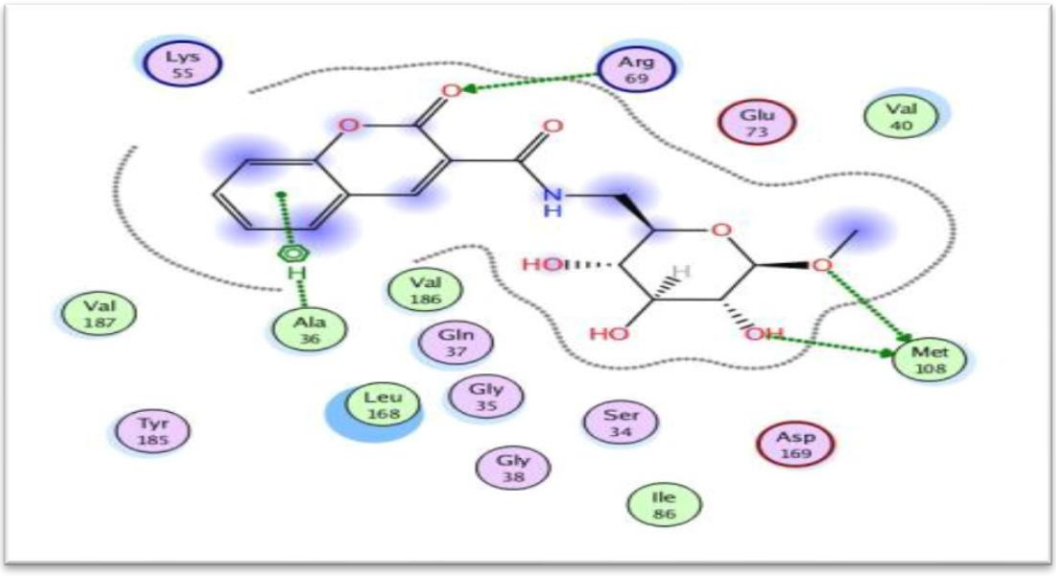

Fig. 7: Compound 7A.

Compound 6B ;
S -7.2428, rmsd-refine 1.8385
Ligand Interactions Report

Ligand	Receptor	Interaction	Distance	E (kcal/mol)
C 30	SD MET 108 (A)	H-donor	4.14	-0.8
6-ring	CB LEU 168 (A)	pi-H	4.47	-0.8
6-ring	CD1 LEU 168 (A)	pi-H	3.78	-0.9

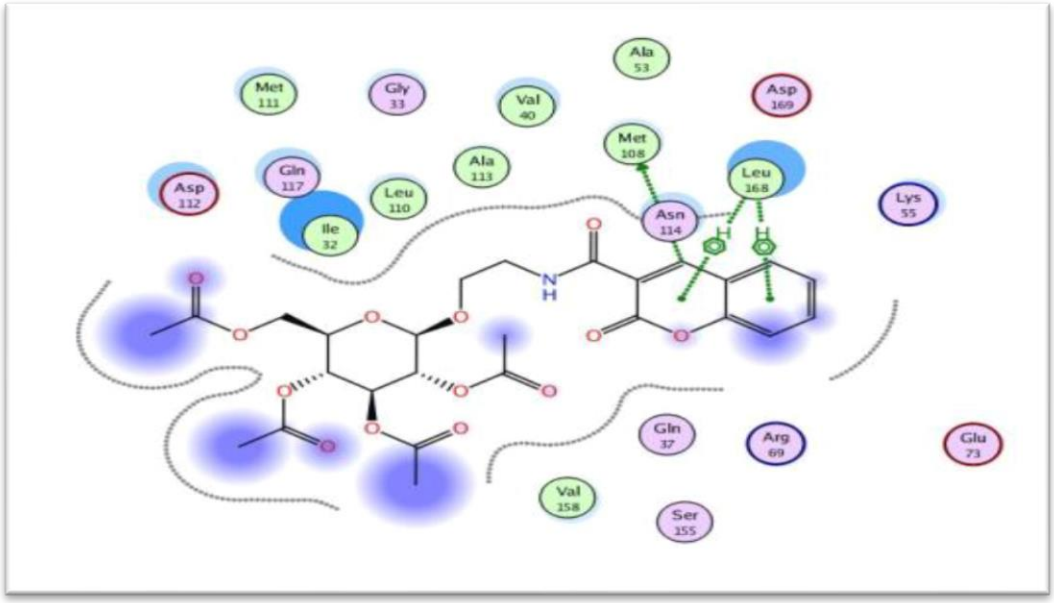

Fig. 8: Compound 6B.

Compound 7B ;
S -5.5211, rmsd-refine 1.3909
Ligand Interactions Report

Ligand	Receptor	Interaction	Distance	E (kcal/mol)
O 8	SD MET 108 (A)	H-donor	3.62	-1.9
O 10	SD MET 108 (A)	H-donor	3.59	-1.2
O 1	NZ LYS 55 (A)	H-acceptor	3.32	-1.9
O 48	N GLN 37 (A)	H-acceptor	3.48	-1.3
O 49	N ALA 36 (A)	H-acceptor	3.20	-1.7

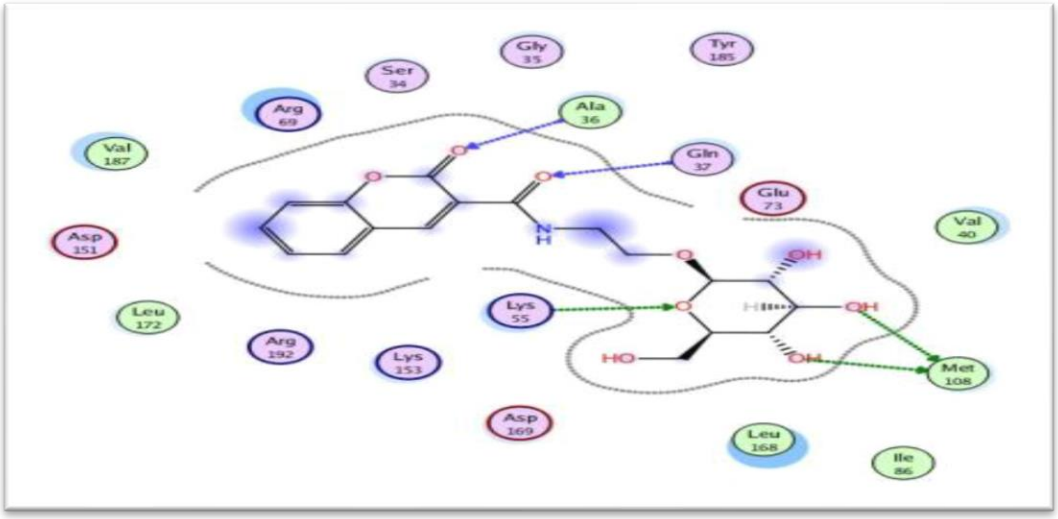

Fig. 9: Compound 7B.

Biological Evaluation:

Cytotoxic Screening:

Determine the Anticancer Activity of 7A Against Liver Carcinoma:

The cytotoxicity potentials of 7A were evaluated by MTT assay against liver cancer primary tissue culture after 48 hr., which appears that 7A exhibited selective cytotoxicity against liver cancer cells isolated from Iraqi patients with inhibitory concentration (IC50) 49.23 µg/ml as shown in Figure (3) and Table (3).

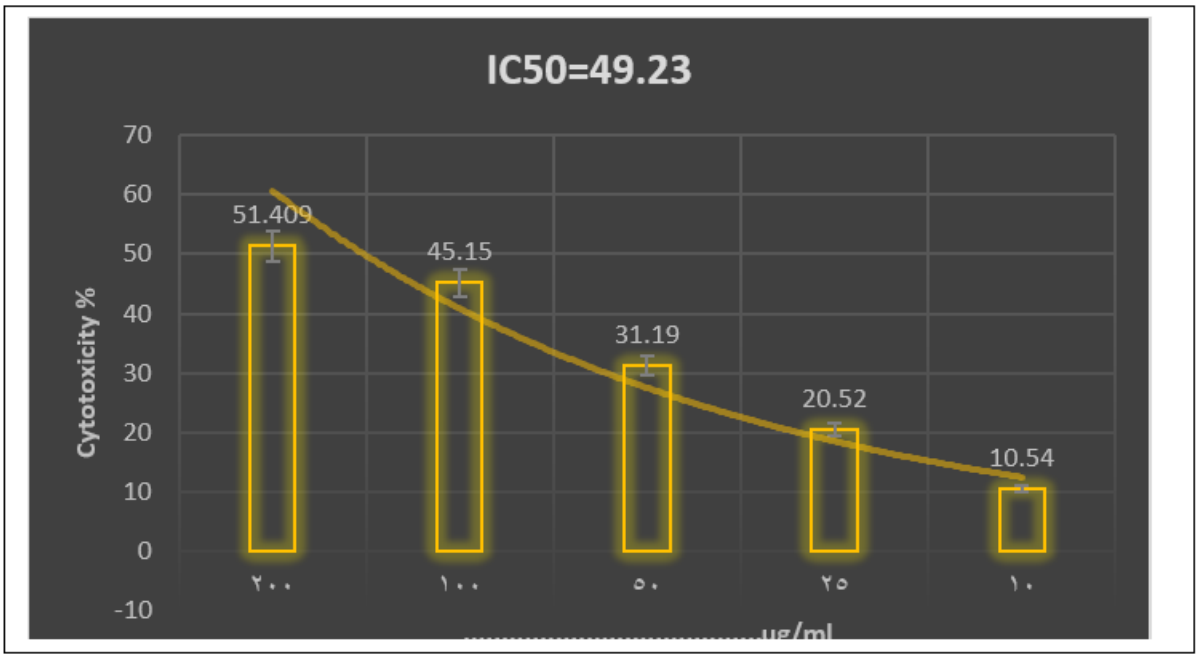

Fig. 10: The cytotoxic effect of 7A (against Human liver cancer cells after 48 hrs of exposure**.**

Table 1: The equation form to calculate the IC50 of 7A against liver cancer cells isolated from Iraqi patients by using AAT Bio-quest website.

IC_{50} Regression Results (Dataset 1)	
Parameter	**Value**
IC_{50}	49.2377
Equations	
Equations	$Y = 43.13 + \frac{93.1512 - 43.13}{1 + \left(\frac{X}{49.2377}\right)^{1.5458}}$
Equation form	$Y = Min + \frac{Max - Min}{1 + \left(\frac{X}{IC50}\right)^{Hill\ coefficient}}$

Determine the Anticancer Activity of 7B Against Liver Carcinoma:

The cytotoxicity potentials of 7B were evaluated by MTT assay against liver cancer primary tissue culture after 48 hr., which appears that 7B exhibited selective cytotoxicity against liver cancer cells isolated from Iraqi patients with inhibitory concentration (IC50) 86.49 µg/ml as showed in Figure (5) and Table (2).

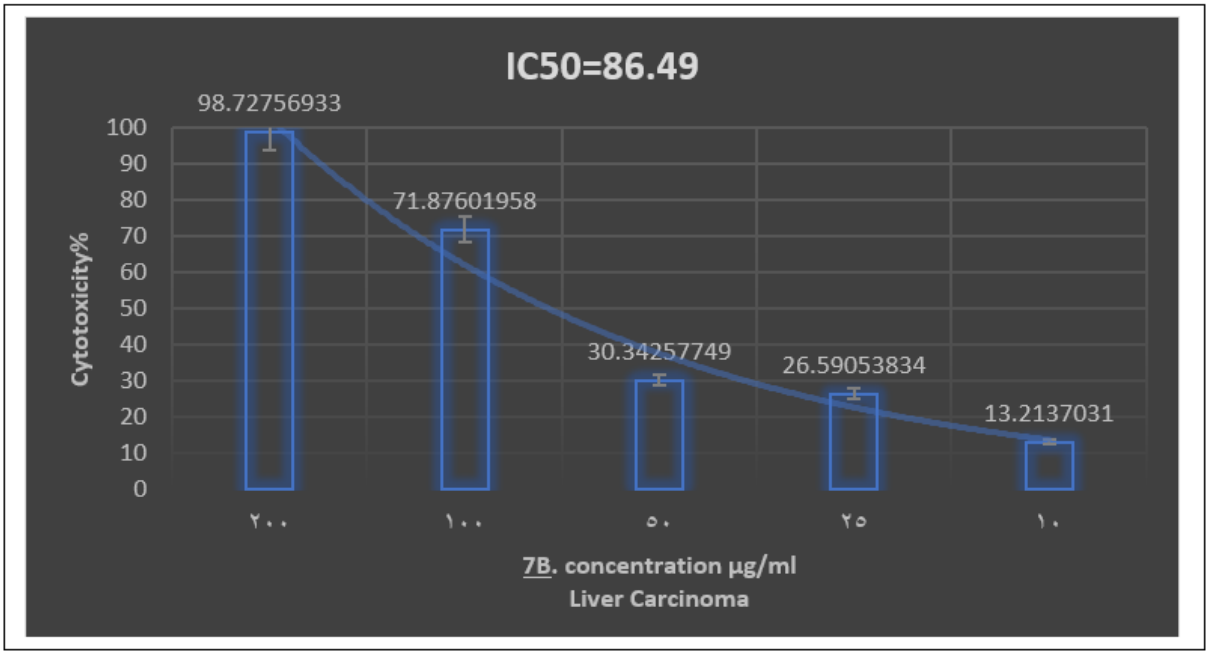

Fig.11: The cytotoxic effect of 7B (against Human liver cancer cells after 48 hrs of exposure.

Table 2: The equation form to calculate the IC50 of 7B against liver cancer cells isolated from Iraqi patients by using AAT Bio-quest website.

IC_{50} Regression Results (Dataset 1)	
Parameter	**Value**
IC_{50}	86.4902
Equations	
Equations	$Y = -6.0522 + \frac{82.231 + 6.0522}{1 + \left(\frac{X}{86.4902}\right)^{2.9133}}$
Equation form	$Y = Min + \frac{Max - Min}{1 + \left(\frac{X}{IC50}\right)^{Hill\ coefficient}}$

The Determination of The Effect of 7A &7B on Apoptosis (DNA Fragmentation) by Using the Acridine-Orange / Ethidium Bromide (AO/EB) Technique:

The fluorescence microscope image of the primary cell culture of human liver cancer cells stained with AO / EtBr and representing the apoptosis method.as show in Figure (10).

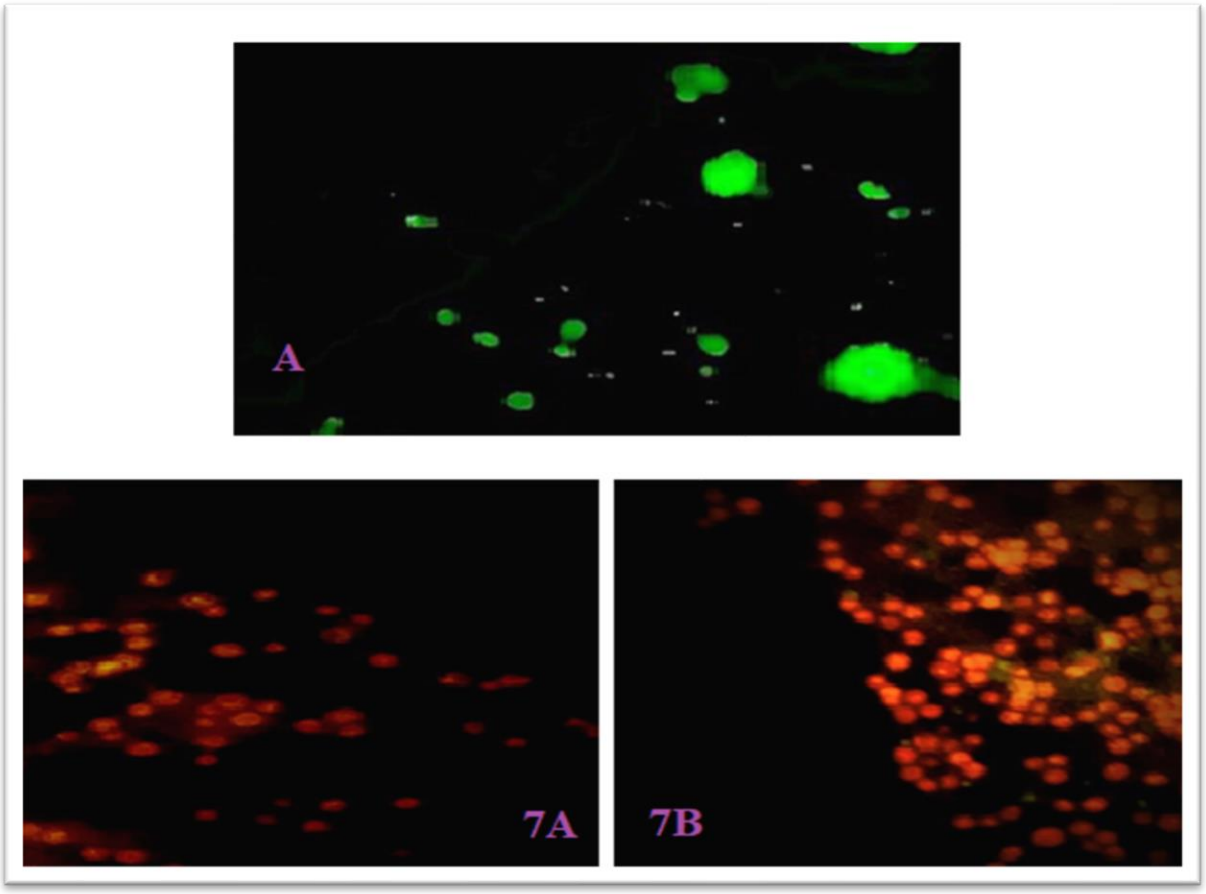

Fig.10: Show (A)Untreated liver cancer cells (100x). (7A) treatment of liver cancer cells with 200ug/ml from 7A after 48 h (100 x), (7B) treatment of liver cancer cells with 200ug/ml from 7 B after 48 h (100 x).

CONCLUSION

A series of new coumarin derivatives containing amide bonds with monosaccharide derivatives. The synthesized compound 7A & 7B showed excellent anti-cancer activity.

REFERENCES

Amabilino, D. B., Smith, D. K., & Steed, J. W. (2017). Supramolecular materials. *Chemical Society Reviews*, *46*(9), 2404–2420.

Bryan, M. C., Dunn, P. J., Entwistle, D., Gallou, F., Koenig, S. G., Hayler, J. D., Hickey, M. R., Hughes, S., Kopach, M. E., & Moine, G. (2018). Key Green Chemistry research areas from a pharmaceutical manufacturers' perspective revisited .*Green Chemistry*, *20*(22), 5082–5103.

de Oliveira, R. N., Cottier, L., Sinou, D., & Srivastava, R. M. (2005). Stereocontrolled palladium (0)-catalyzed preparation of unsaturated azidosugars: An easy access to 2-and 4-aminoglycosides. *Tetrahedron*, *61*(34), 8271–8281.

Du, X., Zhou, J., & Xu, B. (2014). Supramolecular hydrogels made of basic biological building blocks. *Chemistry–An Asian Journal*, *9*(6), 1446–1472.

El-Abid, J., Moreau, V., Kovensky, J., & Chagnault, V. (2021). Effects of CoCl2 on the regioselective tosylation of oligosaccharides. *Journal of Molecular Structure*, *1241*, 130609.

El-Sayed, W. A., Alminderej, F. M., Mounier, M. M., Nossier, E. S., Saleh, S. M.,

& Kassem, A. F. (2022). Novel 1, 2, 3-Triazole-Coumarin Hybrid Glycosides and Their Tetrazolyl Analogues: Design, Anticancer Evaluation and Molecular Docking Targeting EGFR, VEGFR-2 and CDK-2. *Molecules*, *27*(7), 2047.

Emami, S., & Dadashpour, S. (2015). Current developments of coumarin-based anti-cancer agents in medicinal chemistry. *European Journal of Medicinal Chemistry*, *102*, 611–630.

Fattahi, N., Ayubi, M., & Ramazani, A. (2018). Amidation and esterification of carboxylic acids with amines and phenols by N, N′-diisopropylcarbodiimide: A new approach for amide and ester bond formation in water. *Tetrahedron*, *74*(32), 4351–4356.

Gerber, D. E. (2008). Targeted therapies: a new generation of cancer treatments. *American Family Physician*, *77*(3), 311–319.

Hao, S., Cheng, X., Wang, X., An, R., Xu, H., Guo, M., Li, C., Wang, Y., Hou, Z., & Guo, C. (2020). Design, synthesis and biological evaluation of novel carbohydrate-based sulfonamide derivatives as antitumor agents. *Bioorganic Chemistry*, *104*, 104237.

Markad, D., Khullar, S., & Mandal, S. K. (2020). A Primary Amide-Functionalized Heterogeneous Catalyst for the Synthesis of Coumarin-3-carboxylic Acids via a Tandem Reaction. *Inorganic Chemistry*, *59*(16), 11407–11416.

Mohammed, A. I., Mansour, N. H., & Mahdi, L. S. (2017). Synthesis and antibacterial activity of 1-N-(β-d-glucopyranosyl)-4-((1-substituted-1H-1, 2, 3-triazol-4-yl) ethoxymethyl)-1, 2, 3-triazoles. *Arabian Journal of Chemistry*, *10*, S3508–S3514.

Okesola, B. O., & Smith, D. K. (2016). Applying low-molecular weight supramolecular gelators in an environmental setting–self-assembled gels as smart materials for pollutant removal. *Chemical Society Reviews*, *45*(15), 4226–4251.

Pitzer, J., & Steiner, K. (2016). Amides in nature and biocatalysis. *Journal of Biotechnology*, *235*, 32–46.

Ramachandran, P. V., & Hamann, H. J. (2021). Ammonia-borane as a Catalyst for the Direct Amidation of Carboxylic Acids. *Organic Letters*, *23*(8), 2938–2942.

Salar, U., Khan, K. M., Fakhri, M. I., Hussain, S., Tauseef, S., Ameer, S., Wadood, A., Khan, H., & Perveen, S. (2018). 1, 1'-Carbonyldiimidazole (CDI) mediated facile synthesis, structural characterization, antimicrobial activity, and in-silico studies of coumarin-3-carboxamide derivatives. *Medicinal Chemistry*, *14*(1), 86–101.

Wang, Z. D., Mo, Y., Chiou, C.-L., & Liu, M. (2010). A simple preparation of 2, 3, 4, 6-tetra-O-acyl-gluco-, galacto-and mannopyranoses and relevant theoretical study. *Molecules*, *15*(1), 374–384.

Yarlagadda, V., Konai, M. M., Manjunath, G. B., Ghosh, C., & Haldar, J. (2015). Tackling vancomycin-resistant bacteria with 'lipophilic–vancomycin –carbohydrate conjugates.' *The Journal of Antibiotics*, *68*(5), 302–312.

Zhou, J., Li, J., Du, X., & Xu, B. (2017). Supramolecular biofunctional materials. *Biomaterials*, *129*, 1–27.